

DIRECT PREFERENCE OPTIMIZATION FOR SPEECH AUTOREGRESSIVE DIFFUSION MODELS

Zhijun Liu¹, Dongya Jia⁴, Xiaoqiang Wang⁴, Chenpeng Du⁴, Shuai Wang^{3,†}, Zhuo Chen⁴, Haizhou Li²

¹School of Data Science, The Chinese University of Hong Kong, Shenzhen

²School of Artificial Intelligence, The Chinese University of Hong Kong, Shenzhen

³Nanjing University ⁴ByteDance Seed

ABSTRACT

Autoregressive diffusion models (ARDMs) have recently been applied to speech generation, achieving state-of-the-art (SOTA) performance in zero-shot text-to-speech. By autoregressively generating continuous speech tokens with next-token diffusion, these models offer a promising alternative to next-token prediction, avoiding the technical complexities associated with discrete speech tokenization. As a relatively new paradigm, research on reinforcement learning (RL)-based fine-tuning of speech ARDMs remains limited. In this paper, we propose Autoregressive Diffusion-Direct Preference Optimization (ARDM-DPO) to advance this research. By fine-tuning the recently proposed zero-shot text-to-speech model DiTAR with DPO, we achieve significant improvements in terms of speech expressiveness and robustness for long texts.

Index Terms— zero-shot text-to-speech, preference alignment

1. INTRODUCTION

A growing body of work in multimodal generation, including audio [1–3], image [4–6], and video synthesis [7–9], now employs autoregressive diffusion models (ARDMs) as the underlying architecture. ARDMs encode continuous modalities into sequences of continuous latent vectors (“continuous tokens”) and synthesize sequences by autoregressively predicting the next token with a diffusion model. Compared to next-token prediction over discrete token sequences [10, 11], this next-token diffusion approach [12] preserves fine details while avoiding excessively long sequences, thanks to the compactness of continuous latent representations. Notably, recent studies [2, 12–14] applying ARDMs to speech generation report state-of-the-art zero-shot text-to-speech (TTS) performance.

Modern TTS systems trained on large datasets can sample from the data distribution with high fidelity. However, the generated speech may not always align with human preferences after pre-training. For example, when prompted with emotional speech, TTS models can still produce undesirable monotone outputs, requiring additional post-filtering by users [15]. Preference alignment algorithms [16–18] bias the output distribution of generative models toward human-preferred samples, making them an essential post-training step for powerful speech generation systems [19–29].

Direct Preference Optimization [17] (DPO) was originally proposed for aligning language models and was later adapted for fine-tuning diffusion models [30]. In this work, we extend DPO to ARDMs (ARDM-DPO) and apply it to fine-tune the recently proposed DiTAR model [2], which achieves state-of-the-art performance in zero-shot TTS. DiTAR features a highly efficient ARDM

architecture that separates computation for encoding the generation history from denoising the next token. To our knowledge, this is the first preference-alignment method tailored to ARDMs for TTS.

We evaluate ARDM-DPO on two benchmarks: (A) F0 variance for expressiveness and (B) text likelihood for robustness on hard texts challenging autoregressive TTS. ARDM-DPO nearly doubles F0 variance with minimal speaker-similarity loss and reduces CER by 25%. Audio samples and further details can be found in the online supplement¹.

2. BACKGROUND

2.1. Diffusion Models

Suppose $q(x_0)$ is the data distribution. For each diffusion time index $t \in \{1, \dots, T\}$, define the positive decreasing sequence $(\alpha_t)_{t=1}^T$ and the positive increasing sequence $(\sigma_t)_{t=1}^T$. For each t define the Gaussian perturbation distribution $q(x_t|x_0) := \mathcal{N}(x_t; \alpha_t x_0, \sigma_t^2 I_d)$. Define the noise perturbed distribution for each $t \in \{1, \dots, T\}$ as

$$q(x_t) := \int q(x_0)q(x_t|x_0)dx_0. \quad (1)$$

A well-trained diffusion model can be considered as a score estimator $\nabla_{x_t} \log q(x_t)$ trained with denoising score matching [31]. In the DDPM [32, 33] sampler, the diffusion model generates samples starting from random noise $x_T \sim p(x_T) = \mathcal{N}(x_T; 0, I)$. Then it samples x_{t-1} given x_t iteratively.

$$x_{t-1} = a_t x_t + b_t \nabla_{x_t} \log q(x_t) + c_t \epsilon, \quad (2)$$

where $\epsilon \sim \mathcal{N}(0, I)$ is an independent noise, $(a_t)_{t=1}^T$, $(b_t)_{t=1}^T$ and $(c_t)_{t=1}^T$ are positive sequences depending on $(\alpha_t)_{t=1}^T$ and $(\sigma_t)_{t=1}^T$.

2.2. Autoregressive Diffusion Models

For simplicity, we assume that the ARDM always generates N continuous tokens. The ARDM sampling process can be viewed as a Markov chain, as illustrated in Fig. 1. Each state s_n^t is indexed by the pair $(n, t) \in \{1, \dots, N\} \times \{1, \dots, T\}$, where n is the token index and t is the diffusion time index. Each state s_n^t contains the history tokens already denoised $x_{<n}^0$ and the current noisy token x_n^t that is being denoised, where we define $x_{<n}^0 := x_{1..n-1}^0$.

Given the state s_n^t , an ARDM estimates the conditional score $\nabla \log q(x_n^t|x_{<n}^0)$ and transitions from s_n^t to s_n^{t-1} when $t > 1$. Upon reaching state s_n^T , where a token is fully denoised, a random Gaussian noise x_{n+1}^T is sampled, and a new DDPM sampling process starts from state $s_{n+1}^T = (x_{<n}^0, x_{n+1}^T)$.

[†]: Corresponding author

¹<https://zjlww.github.io/ardm-dpo/>

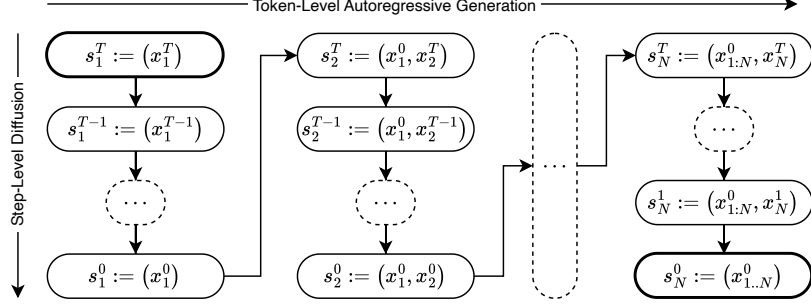


Fig. 1. ARDM sampling viewed as a Markov chain. Each state contains both the history-generated tokens and the current noisy token. In this work, we define $x_{a:b} := \{x_n : a \leq n < b, n \in \mathbb{Z}\}$ and $x_{a..b} := \{x_n : a \leq n \leq b, n \in \mathbb{Z}\}$.

3. ARDM-DPO

Let \mathbf{x} denote an ARDM sampling trajectory that contains all intermediate states in Fig. 1. The reward function $r(x_{1..N}^0)$ is defined over the terminal states. For a trajectory \mathbf{x} , we define $r(\mathbf{x}) := r(x_{1..N}^0)$. Consider the following KL divergence-constrained policy optimization problem:

$$\max_{\pi} [\mathbb{E}_{\pi(\mathbf{x})} [r(\mathbf{x})] - \beta D_{\text{KL}}(\pi(\mathbf{x}) \parallel \mu(\mathbf{x}))], \quad (3)$$

where $\beta > 0$ is the weight of the KL constraint. The KL-divergence constraint ensures that the learned policy $\pi(\mathbf{x})$ does not deviate too far from the reference distribution $\mu(\mathbf{x})$. The unique optimal policy π_r given reward r is [17, 34]:

$$\pi_r(\mathbf{x}) := \frac{1}{Z_r} \mu(\mathbf{x}) \exp \left(\frac{1}{\beta} r(\mathbf{x}) \right), \quad (4)$$

where Z_r is defined as $Z_r := \int \mu(\mathbf{x}) \exp \left(\frac{1}{\beta} r(\mathbf{x}) \right) d\mathbf{x}$. Then, we have:

$$r(\mathbf{x}) = \beta \log \frac{\pi_r(\mathbf{x})}{\mu(\mathbf{x})} + \beta \log Z_r. \quad (5)$$

Marginalizing over all ARDM intermediate states gives:

$$r(x_{1..N}^0) = \beta \mathbb{E}_{\pi_r(\mathbf{x}|x_{1..N}^0)} \left[\log \frac{\pi_r(\mathbf{x})}{\mu(\mathbf{x})} \right] + \beta \log Z_r. \quad (6)$$

As in DPO, we assume that the log probability of human listeners preferring sample $x_{1..N}^0$ over $y_{1..N}^0$ is modeled by a Bradley-Terry model [17]:

$$\log P(x_{1..N}^0 \succ y_{1..N}^0) = \log \sigma(r(x_{1..N}^0) - r(y_{1..N}^0)). \quad (7)$$

Given a dataset \mathcal{D} of preference pairs, we can estimate the reward model parameters with maximum likelihood estimation:

$$\max_r \mathbb{E}_{x_{1..N}^0, y_{1..N}^0 \sim \mathcal{D}} [\log P(x_{1..N}^0 \succ y_{1..N}^0)]. \quad (8)$$

As a result of Eq. (6), optimizing the reward model r with maximum likelihood can be conducted without an explicit reward model by optimizing:

$$\mathbb{E}_{x_{1..N}^0, y_{1..N}^0 \sim \mathcal{D}} [\mathcal{J}(x_{1..N}^0, y_{1..N}^0)], \quad (9)$$

where

$$\begin{aligned} \mathcal{J}(x_{1..N}^0, y_{1..N}^0) := & \log \sigma(TN\beta \cdot \mathbb{E}_{\substack{\mathcal{U}(t), \mathcal{U}(n) \\ \pi(x_n^t, x_n^{t-1} | x_{\leq n}^0) \\ \pi(y_n^t, y_n^{t-1} | y_{\leq n}^0)}} [\ell_n^t(\mathbf{x}) - \ell_n^t(\mathbf{y})]), \end{aligned} \quad (10)$$

with $\ell_n^t(\mathbf{x})$ defined as:

$$\ell_n^t(\mathbf{x}) := \log \frac{\pi(x_n^{t-1} | x_n^t, x_{\leq n}^0)}{\mu(x_n^{t-1} | x_n^t, x_{\leq n}^0)}. \quad (11)$$

As proposed in Diffusion-DPO [30], we assume that the distribution $\pi(x_n^t, x_n^{t-1} | x_{\leq n}^0)$ can be approximated with $q(x_n^t | x_n^0) \cdot q(x_n^{t-1} | x_n^t, x_n^0)$. We also move the expectation over $\mathcal{U}(t)$, $q(x_n^t | x_n^0)$, and $q(y_n^t | y_n^0)$ from the inside of $\log \sigma$ to the outside with Jensen's inequality to obtain the approximate lower bound \mathcal{L} for \mathcal{J} . The constant factor TN is absorbed into β in Eq. (12). $\mathcal{U}(t), \mathcal{U}(n)$ are uniform distributions over all possible values.

$$\begin{aligned} \mathcal{J}(x_{1..N}^0, y_{1..N}^0) &\geq \mathcal{L}(x_{1..N}^0, y_{1..N}^0) := \\ &\mathbb{E}_{\substack{\mathcal{U}(t) \\ q(x_n^t | x_n^0) \\ q(y_n^t | y_n^0)}} \left[\log \sigma \left(\beta \mathbb{E}_{\substack{\mathcal{U}(n) \\ q(x_n^{t-1} | x_n^t, x_n^0) \\ q(y_n^{t-1} | y_n^t, y_n^0)}} [\ell_n^t(\mathbf{x}) - \ell_n^t(\mathbf{y})] \right) \right]. \end{aligned} \quad (12)$$

Notice that the expectation $\mathbb{E}_{q(x_n^{t-1} | x_n^t, x_n^0)} [\ell_n^t(\mathbf{x})]$ can be written as the difference of KL divergences:

$$\begin{aligned} &D_{\text{KL}}(q(x_n^{t-1} | x_n^t, x_n^0) \parallel \mu(x_n^{t-1} | x_n^t, x_{\leq n}^0)) \\ &- D_{\text{KL}}(q(x_n^{t-1} | x_n^t, x_n^0) \parallel \pi(x_n^{t-1} | x_n^t, x_{\leq n}^0)). \end{aligned} \quad (13)$$

Without loss of generality, suppose that the ARDM is trained with the denoising objective. Then Eq. (13) is equivalent to:

$$\omega_t (-\|v_\theta(x_n^t, x_{\leq n}^0) - x_n^0\|_2^2 + \|v_{\text{ref}}(x_n^t, x_{\leq n}^0) - x_n^0\|_2^2), \quad (14)$$

where ω_t is a time-dependent weight. Finally, we arrive at the ARDM-DPO training objective:

$$\begin{aligned} \mathcal{L}(x_{1..N}^0, y_{1..N}^0) := & \mathbb{E}_{\substack{\mathcal{U}(t) \\ q(x_n^t | x_n^0) \\ q(y_n^t | y_n^0)}} \left[\log \sigma \left(\beta \omega_t \mathbb{E}_{\mathcal{U}(n)} \right. \right. \\ & \left. \left. - \|v_\theta(x_n^t, x_{\leq n}^0) - x_n^0\|_2^2 + \|v_{\text{ref}}(x_n^t, x_{\leq n}^0) - x_n^0\|_2^2 \right. \right. \\ & \left. \left. + \|v_\theta(y_n^t, y_{\leq n}^0) - y_n^0\|_2^2 - \|v_{\text{ref}}(y_n^t, y_{\leq n}^0) - y_n^0\|_2^2 \right) \right]. \end{aligned} \quad (15)$$

The DiTAR model used in our experiments is based on v -prediction, with continuous time $t \in [0, 1]$ where $t = 1$ corresponds to pure noise. We can derive the ARDM-DPO training objective for DiTAR as follows:

$$\begin{aligned} \mathcal{L}(x_{1..N_x}^0, y_{1..N_y}^0) := & \mathbb{E}_{\substack{t \sim \mathcal{U}(0,1) \\ x_{1..N_x}^t \sim \text{i.i.d. } \mathcal{N}(0, I) \\ y_{1..N_y}^t \sim \text{i.i.d. } \mathcal{N}(0, I)}} \left[\log \sigma \left(\right. \right. \\ & d^{-1} \beta \mathbb{E}_n \left[\|v_{\text{ref}}(x_n^t, x_{\leq n}^0) - x_n^t\|_2^2 - \|v_\theta(x_n^t, x_{\leq n}^0) - x_n^t\|_2^2 \right] \\ & \left. \left. - d^{-1} \beta \mathbb{E}_n \left[\|v_{\text{ref}}(y_n^t, y_{\leq n}^0) - y_n^t\|_2^2 - \|v_\theta(y_n^t, y_{\leq n}^0) - y_n^t\|_2^2 \right] \right) \right]. \end{aligned} \quad (16)$$

where $x_n^t = \alpha_t x_n^0 + \sigma_t x_n^1$ and $\dot{x}_n^t = \dot{\alpha}_t x_n^0 + \dot{\sigma}_t x_n^1$. y_n^t and \dot{y}_n^t are defined similarly. We dropped the time-dependent weight ω_t following the practice in Diffusion-DPO. In Eq. (16) we compute \mathbb{E}_n separately for \mathbf{x} and \mathbf{y} , since the two trajectories can have different lengths N_x and N_y . We normalized β with $d^{-1} = 1/256$ in our experiments, with d the dimensionality of each token in DiTAR.

4. EXPERIMENTS

4.1. Common Setup

Base Model. We fine-tuned a base DiTAR model with 0.4B parameters, pretrained on an internal corpus of around 280,000 hours of Chinese and English audio. The LM in the base model has 24 Transformer blocks, and the diffusion head contains 4 blocks. Each Transformer block has 1024 hidden dimensions and 16 attention heads.

Inference. We used the same diffusion sampler for training sample generation and model evaluation. We use a 16-step DDPM sampler with a linear time schedule. We enabled LM Guidance [2], which is similar to classifier-free guidance (CFG), with weight $w = 2$.

DPO Training. All experiments were carried out on 32 A100 GPUs, with a local batch size of 1 pair and gradient accumulation of 32 steps. The effective batch size is 1024 pairs. We used the AdamW optimizer, with a fixed learning rate of 2×10^{-6} , weight decay 0.01, $\beta_1 = 0.9$, $\beta_2 = 0.95$.

Objective Evaluations. In all experiments, we report the word error rate (WER) using Whisper-large-v3 for English and the character error rate (CER) using Paraformer-zh for Chinese. Additionally, we calculate the cosine similarity of speaker embeddings (SIM) between the prompt and the generated audio using the WavLM-TDCNN model. All metrics were computed using Seed-TTS-Eval². We also report the token average KL divergence on the test set, which is defined as

$$d^{-1} \mathbb{E}_{\substack{\pi(\mathbf{x}), \mathcal{U}(n) \\ \mathcal{U}(t), q(x_n^t | x_n^0)}} \|v_\theta(x_n^t, x_{<n}^0) - v_{\text{ref}}(x_n^t, x_{<n}^0)\|_2^2, \quad (17)$$

as a measure of the divergence between the fine-tuned model π_θ and the reference model μ . For each objective metric, we report the average value across 8 random runs.

Subjective Evaluations. Twenty listeners participated in pairwise listening tests, comparing audio from two TTS systems (e.g. A and B) on specific aspects (e.g., naturalness). For each pair, listeners chose “A wins”, “B wins”, or “tie”.

4.2. Task A: Improving F0 Variance

Task. The fundamental frequency variance (F0V) is strongly correlated with the perceived expressiveness of the generated speech. Optimizing F0V can effectively prevent the model from producing monotone responses.

Preference Dataset. We randomly sampled speech prompts and texts from the LibriTTS [35] dataset. For each prompt-text pair, we generated 32 candidate responses using the base model. We then measured the F0V of these responses and selected the best and worst in terms of F0V to form a preference pair. In total, we collected 256k preference pairs, amounting to approximately 1,000 hours of speech.

Evaluation Dataset. For evaluation, we randomly selected 38 prompt audios and target texts from different speakers in the LibriTTS test-clean subset.

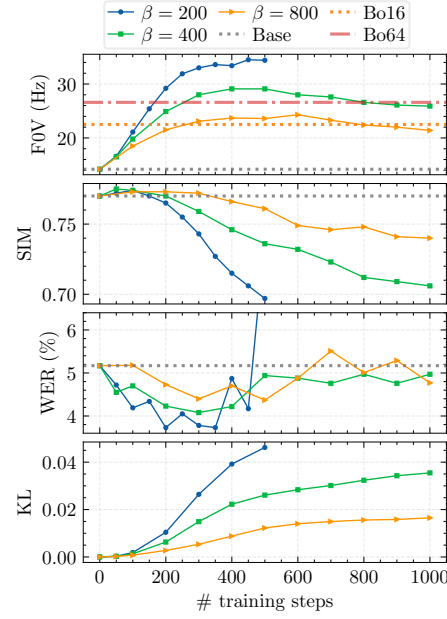


Fig. 2. Trajectories of F0V, SIM, and WER of various models over 1000 training steps for Task A.

Rejection Sampling Fine-Tuning. We compare ARDM-DPO with rejection sampling fine-tuning (RAFT) [36]. RAFT performs supervised fine-tuning (SFT) iteratively. In each RAFT iteration, we collect approximately 1,000 hours of speech continuations from the best policy found in the previous iteration. For each prompt, we sample 32 candidate responses and retain the one with the highest F0V. RAFT experiments use a batch size of 512 and a learning rate of 1×10^{-5} .

Method	F0V \uparrow	SIM \uparrow	WER \downarrow	KL \downarrow
Base Model	14.2	0.770	5.17	—
Best-of-16	22.5	0.770	4.74	—
Best-of-64	26.6	0.770	4.93	—
RAFT ³⁰⁰ steps iter 1	18.3	0.763	5.97	0.057
RAFT ³⁰⁰ steps iter 2	19.7	0.758	5.91	0.230
RAFT ³⁰⁰ steps iter 3	20.1	0.756	5.99	0.237
DPO $\beta = 200$ ²⁰⁰ steps	29.2	0.765	3.73	0.010

Table 1. Selected objective evaluation results for Task A.

Grid Search for Optimal β . In DPO training, β controls the strength of KL regularization. We report results for $\beta \in \{200, 400, 800\}$. The evaluation results can be found in Tab. 1 and Fig. 2. We observe that SIM gradually decreases throughout the training process for all values of β . This decrease is not caused by changes in prosody, as the best-of-K (BoK) sampling results in Tab. 1 indicate that an increase in F0V does not significantly reduce SIM. For larger values of β , the KL constraint is stronger, resulting in less degradation in SIM; however, the improvement in F0V is also smaller. We recommend applying early stopping to prevent significant quality degradation.

Diffusion Loss During DPO. We visualize the changes in diffusion loss for the winning and losing samples (Δ_+, Δ_-) during training with $\beta = 200$ in Fig. 3. Although the training objective in Eq. (16) is supposed to decrease the diffusion loss of the winning samples while increasing the diffusion loss of the losing samples, we observe that the model tends to increase both losses during training. A similar

²<https://github.com/BytedanceSpeech/seed-tts-eval>

phenomenon has been observed in LLM DPO training [37]. Investigating this behavior is left as future work.

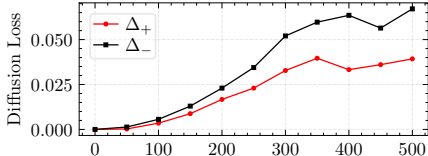


Fig. 3. Change in diffusion loss of the winning and losing samples in Task A DPO with $\beta = 200$.

Subjective Evaluations. For each of the 38 test cases, we generated three random responses from both the base model and the DPO model (200 steps, $\beta = 200$) for comparison. Evaluators assessed the response pairs based on three criteria: naturalness, speaker similarity to the prompt, and expressiveness. As shown in Fig. 4, DPO training slightly reduces naturalness and speaker similarity but significantly enhances perceived expressiveness.

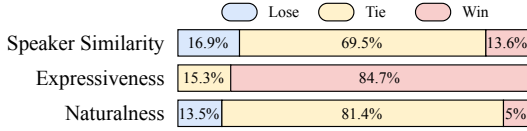


Fig. 4. Results of the subjective evaluation: DPO vs. base model.

4.3. Task B: Improving Text Likelihood

Task. When evaluated on out-of-domain complex texts containing repetitions, autoregressive TTS models often make mistakes in audio-text alignment, such as missing or inserting words. Following prior work, we trained a phoneme-based CTC model [38] and used its negative log likelihood per phoneme (NLL) as a proxy for speech intelligibility. The CTC model consists of 6 transformer blocks, each with a hidden dimension of 1024 and 16 attention heads.

Preference Dataset. The prompts were randomly sampled from DidiSpeech-2 [39], a Chinese speech corpus consisting of 227 hours of recordings from 1,500 speakers. The texts were selected from a dataset of 100,000 long Chinese sentences, with randomly introduced repetitive phrases and clauses. For each prompt-text pair, we generated 16 candidate responses using the base model. We then calculated the CTC loss with our CTC model and selected the best and worst responses to form a preference pair. In total, we collected 430,000 preference pairs, totaling approximately 3,500 hours.

Evaluation Dataset. We utilized the hard test set proposed in Seed-TTS [19], which contains 400 challenging test cases in Chinese with complex text. We excluded all speakers in the Seed-TTS-Eval hard set from the preference dataset, guaranteeing that they remained unseen during training.

Method	NLL \downarrow	SIM \uparrow	CER \downarrow	KL \downarrow
Base Model	0.55	0.711	8.37	—
Best-of-8 (CER)	0.39	0.713	4.99	—
Best-of-8 (NLL)	0.27	0.712	6.79	—
DPO ${}^{9000 \text{ steps}}_{\beta = 1600}$	0.32	0.712	6.32	0.009

Table 2. Selected objective evaluation results for Task B.

Grid Search for Optimal β . We initially experimented with $\beta \in \{200, 400, \dots, 3200, 6400\}$ and observed that $\beta \leq 400$ led to increases in NLL and CER within 300 steps, while $\beta \geq 6400$ resulted

in very slow optimization. Consequently, we focused on $\beta \in \{800, 1600, 3200\}$ for further analysis. The trajectories of NLL, SIM, and CER during training are shown in Fig. 5. We found that the DPO model trained for 9000 steps with $\beta = 1600$ achieved the best performance, with a 25% reduction in CER. Detailed results are provided in Tab. 2.

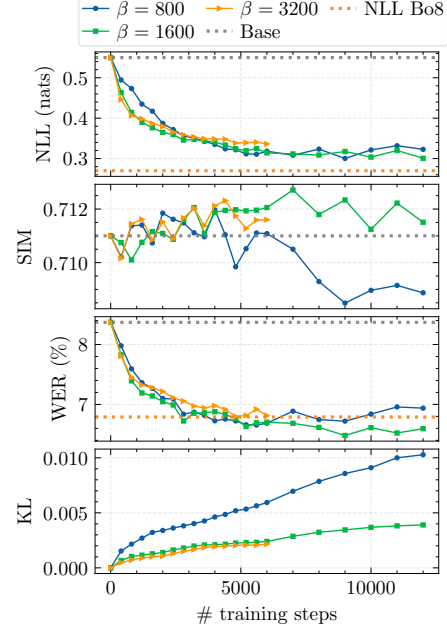


Fig. 5. Trajectories of NLL, SIM, and CER of various models over 12,000 training steps for Task B.

Subjective evaluations. We randomly sampled 40 test cases from the test set and generated three random response pairs for each test case from the base model and the DPO model (9,000 steps, $\beta = 1600$). Evaluators assessed all pairs for naturalness and speaker similarity. We find that the DPO model performs similarly to the base model. For naturalness, the lose/tie/win probabilities are 4.4%, 88.7%, and 6.9%, respectively; for speaker similarity, they are 2.1%, 94.3%, and 3.6%, respectively. This indicates good prior preservation of ARDM-DPO on Task B.

5. CONCLUSIONS AND LIMITATIONS

In this work, we introduced ARDM-DPO, the first direct preference optimization method tailored for autoregressive diffusion TTS. Through comprehensive experiments on DiTAR, we demonstrate that ARDM-DPO achieves significant improvements in speech expressiveness and robustness on challenging long texts while maintaining speaker similarity and speech naturalness.

We observed that ARDM-DPO training on Task A is unstable and requires early stopping to avoid speech quality degradation. The underlying cause warrants further investigation. It is well known that the construction of the preference dataset in DPO plays a critical role in ensuring good performance [20, 21, 40]. We leave these directions for future work.

6. REFERENCES

- [1] Zhijun Liu, Shuai Wang et al., “Autoregressive diffusion transformer for text-to-speech synthesis,” *arXiv preprint arXiv:2406.05551*, 2024.

[2] Dongya Jia, Zhuo Chen et al., “DiTAR: Diffusion transformer autoregressive modeling for speech generation,” in *ICML*, 2025.

[3] Chenyu Yang, Shuai Wang et al., “SongBloom: Coherent song generation via interleaved autoregressive sketching and diffusion refinement,” *arXiv preprint arXiv:2506.07634*, 2025.

[4] Tianhong Li, Yonglong Tian et al., “Autoregressive image generation without vector quantization,” in *NeurIPS*, 2024.

[5] Siqi Kou, Jiachun Jin et al., “Orthus: Autoregressive interleaved image-text generation with modality-specific heads,” in *ICML*, 2025.

[6] NextStep Team, Chunrui Han et al., “NextStep-1: Toward autoregressive image generation with continuous tokens at scale,” *arXiv preprint arXiv:2508.10711*, 2025.

[7] Tianwei Yin, Qiang Zhang et al., “From slow bidirectional to fast autoregressive video diffusion models,” in *CVPR*, 2025.

[8] Haoge Deng, Ting Pan et al., “Autoregressive video generation without vector quantization,” *arXiv preprint arXiv:2412.14169*, 2024.

[9] Hansi Teng, Hongyu Jia et al., “MAGI-1: Autoregressive video generation at scale,” *arXiv preprint arXiv:2505.13211*, 2025.

[10] Yiwei Guo, Zhihan Li et al., “Recent advances in discrete speech tokens: A review,” *arXiv preprint arXiv:2502.06490*, 2025.

[11] Tomoki Hayashi, Shinji Watanabe, “DiscreTalk: Text-to-speech as a machine translation problem,” *arXiv preprint arXiv:2005.05525*, 2020.

[12] Yutao Sun, Hangbo Bao et al., “Multimodal latent language modeling with next-token diffusion,” *arXiv preprint arXiv:2412.08635*, 2024.

[13] Zhiliang Peng, Jianwei Yu et al., “VibeVoice technical report,” *arXiv preprint arXiv:2508.19205*, 2025.

[14] Yanqing Liu, Ruiqing Xue et al., “Next tokens denoising for speech synthesis,” *arXiv preprint arXiv:2507.22746*, 2025.

[15] Xiaoxue Gao, Chen Zhang et al., “Emo-DPO: Controllable emotional speech synthesis through direct preference optimization,” in *ICASSP*, 2025.

[16] Long Ouyang, Jeffrey Wu et al., “Training language models to follow instructions with human feedback,” *NeurIPS*, 2022.

[17] Rafael Rafailov, Archit Sharma et al., “Direct Preference Optimization: Your language model is secretly a reward model,” in *NeurIPS*, 2023.

[18] Jiazheng Xu, Xiao Liu et al., “ImageReward: Learning and evaluating human preferences for text-to-image generation,” in *NeurIPS*, 2023.

[19] Philip Anastassiou, Jiawei Chen et al., “Seed-TTS: A family of high-quality versatile speech generation models,” *arXiv preprint arXiv:2406.02430*, 2024.

[20] Jinchuan Tian, Chunlei Zhang et al., “Preference alignment improves language model-based TTS,” in *ICASSP*, 2025.

[21] Xueyao Zhang, Yuancheng Wang et al., “Advancing zero-shot text-to-speech intelligibility across diverse domains via preference alignment,” in *ACL*, 2025.

[22] Zhihao Du, Changfeng Gao et al., “CosyVoice 3: Towards in-the-wild speech generation via scaling-up and post-training,” *arXiv preprint arXiv:2505.17589*, 2025.

[23] Yinghao Aaron Li, Rithesh Kumar et al., “DMOSpeech: Direct metric optimization via distilled diffusion model in zero-shot speech synthesis,” in *ICML*, 2025.

[24] Yuchen Hu, Chen Chen et al., “Robust zero-shot text-to-speech synthesis with reverse inference optimization,” *arXiv preprint arXiv:2407.02243*, 2024.

[25] Dong Zhang, Zhaowei Li et al., “SpeechAlign: Aligning speech generation to human preferences,” *NeurIPS*, 2024.

[26] Chen Chen, Yuchen Hu et al., “Enhancing zero-shot text-to-speech synthesis with human feedback,” *arXiv preprint arXiv:2406.00654*, 2024.

[27] Jingyi Chen, Ju Seung Byun et al., “Fine-tuning text-to-speech diffusion models using reinforcement learning with human feedback,” in *Interspeech*, 2025.

[28] Jixun Yao, Yuguang Yang et al., “Fine-grained preference optimization improves zero-shot text-to-speech,” *arXiv preprint arXiv:2502.02950*, 2025.

[29] Kangxiang Xia, Xinfu Zhu et al., “MPO: Multidimensional preference optimization for language model-based text-to-speech,” *arXiv preprint arXiv:2509.00685*, 2025.

[30] Bram Wallace, Meihua Dang et al., “Diffusion model alignment using direct preference optimization,” in *CVPR*, 2024.

[31] Yang Song, Jascha Sohl-Dickstein et al., “Score-based generative modeling through stochastic differential equations,” in *ICLR*, 2021.

[32] Jonathan Ho, Ajay Jain et al., “Denoising diffusion probabilistic models,” in *NeurIPS*, 2020.

[33] Jiaming Song, Chenlin Meng et al., “Denoising diffusion implicit models,” in *ICLR*, 2021.

[34] Xue Bin Peng, Aviral Kumar et al., “Advantage-weighted regression: Simple and scalable off-policy reinforcement learning,” *arXiv preprint arXiv:1910.00177*, 2019.

[35] Heiga Zen, Viet Dang et al., “LibriTTS: A corpus derived from librispeech for text-to-speech,” in *Interspeech*, 2019.

[36] Hanze Dong, Wei Xiong et al., “RAFT: Reward rAnked Fine-Tuning for generative foundation model alignment,” *TMLR*, 2023.

[37] Yuzi Yan, Yibo Miao et al., “3D-Properties: Identifying challenges in dpo and charting a path forward,” in *ICLR*, 2025.

[38] Alex Graves, Santiago Fernández et al., “Connectionist Temporal Classification: labelling unsegmented sequence data with recurrent neural networks,” in *ICML*, 2006.

[39] Tingwei Guo, Cheng Wen et al., “DiDiSpeech: A large scale mandarin speech corpus,” in *ICASSP*, 2021.

[40] Navonil Majumder, Chia-Yu Hung et al., “Tango 2: Aligning diffusion-based text-to-audio generations through direct preference optimization,” *arXiv preprint arXiv:2404.09956*, 2024.